

Semiarid mangrove species classification using machine learning algorithms and visible UAV data

E Torres-Aguirre^a, F Flores-de-Santiago^{*a}, L Valderrama-Landeros^b, F Amezcua^c & F Flores-Verdugo^c

^aUnidad Académica Procesos Oceánicos y Costeros, Instituto de Ciencias del Mar y Limnología, Universidad Nacional Autónoma de México, Mexico City - 04510, Mexico

^bCoordinación de Geomática, Comisión Nacional Para el Conocimiento y Uso de la Biodiversidad, Mexico City - 14010, Mexico

^cUnidad Académica Mazatlán, Instituto de Ciencias del Mar y Limnología, Universidad Nacional Autónoma de México, Mazatlán - 82040, Mexico

*[E-mail: ffloresd@comarl.unam.mx]

Received 20 January 2024; revised 13 February 2024

Remote sensing studies have emerged as a crucial tool for monitoring and managing mangrove forests, with Unmanned Aerial Vehicles (UAV) being a popular platform for data collection. UAV surveys offer a non-invasive and efficient means of gathering high-resolution data on mangrove forests, enabling detailed analysis of their structure and health. However, the cost of UAV platforms and software can be a major drawback, particularly for small-scale projects. Despite these difficulties, this research provides valuable insights as it aimed to assess seasonal variations in mangrove forest vegetation at a local scale during the winter, dry, and rainy seasons utilizing solely visible data from a conventional UAV camera and processed through three machine learning algorithms and an 11×11 Lee Sigma speckle filter. The Support Vector Machine (SVM) algorithm outperformed the Random Forest (RF) and Neural Network (NN) algorithms in terms of overall accuracy during the dry season. Specifically, the SVM algorithm achieved an accuracy of 85 % for the dry, 61 % for the winter, and 57 % for the rainy season. In comparison, the RF algorithm achieved accuracies of 80 % for the dry, 77 % for the rainy, and 63 % for the winter season, and the NN algorithm recorded accuracies of 71 % for the dry, 65 % for the rainy, and 57 % for the winter season. These findings indicate that the SVM algorithm is a more effective approach for the dry season. Importantly, this study demonstrates the potential of machine learning algorithms in classifying mangrove species using visible UAV data, which could substantially enhance the efficiency and cost-effectiveness of mangrove forest management.

[**Keywords:** Artificial neural networks, DJI phantom, Mexico, Pixel-level, Random forest, Support vector machine]

Introduction

Mangrove forests are diverse trees and shrubs that thrive in the hypersaline intertidal zone, where they are exposed to saltwater from the ocean and freshwater from rivers¹. Mangroves possess a complex root system that enables them to anchor themselves in the soft, muddy soil and filter out excess salt from the water they absorb². Mangroves are home to a wide range of plant and animal species in tropical and arid/semiarid regions, many of which are exclusive to this ecosystem³. For instance, they provide a habitat for a variety of fish, crustaceans, and mollusks, as well as for birds and mammals⁴. They serve as a natural barrier against coastal erosion and storm surges, safeguarding coastlines and the communities that depend on them⁵. Also, mangrove forests are crucial in carbon sequestration, contributing to climate change mitigation⁶.

Mangrove forests are facing a major threat from human activities, including deforestation, pollution, and climate change⁷. Remote sensing techniques have been increasingly employed in recent decades to better comprehend and monitor the health of these forests⁸. The technique involves the use of satellite or airborne sensors to gather data on the physical and biological characteristics of the forest, such as vegetation cover, biomass, and species composition⁹. This data can then map and monitor forest changes over time and inform conservation and management efforts¹⁰.

Unmanned Aerial Vehicles (UAVs), known as drones, have emerged as a promising tool for studying mangrove forests¹¹. These platforms are equipped with high-resolution sensors that can capture detailed images and data, enabling researchers to map and monitor the health and extent of mangrove forests with greater accuracy and efficiency¹². In addition,

UAV surveys can provide valuable insights into the ecological processes of these ecosystems, such as changes in vegetation cover, water quality, and sedimentation patterns¹³. As such, they have the potential to inform and guide conservation efforts aimed at protecting and restoring mangrove forests¹⁴.

UAVs have become increasingly popular, but their cost can be a substantial disadvantage. The price of a UAV can range from a few hundred to several thousand US dollars, depending on the model and sensors employed¹⁵. This high cost can be a hindrance for many individuals and institutions that may not have the budget to invest in a UAV. Additionally, the cost of repairs and maintenance can add up over time, making it difficult for some to justify the expense. The risk of damage or loss can be another concern, as replacing or repairing a UAV can be costly. Moreover, the UAVs' ultra-high spatial resolution (cm/pixel) presents some disadvantages, such as a large amount of generated data. This situation could be overwhelming for storage and processing, leading to longer computing times¹⁶.

UAV studies commonly employ two methods for land cover analysis: pixel-based and object-based classifications¹⁷. The pixel-based approach assigns a land cover class to each pixel in an image based on spectral characteristics. On the other hand, object-based classification groups adjacent pixels with similar spectral characteristics into objects and assigns a land cover class to each object¹⁸. While pixel-based classification is simpler and faster, it has been suggested that it may not accurately capture the spatial variability of land cover features. Object-based classification, on the other hand, can better capture the spatial variability of land cover features, but it requires more computational resources and may be more time-consuming¹⁹. Ultimately, the choice between pixel-based and object-based classification depends on the specific research question, the characteristics of the study area, and the available budget.

The salt-and-pepper noise is a common UAV issue in pixel-based studies with some disadvantages. This effect occurs when individual pixels in an image are misclassified, resulting in scattered areas of incorrect data²⁰. This can be particularly problematic in areas with complex land cover, such as mangrove forests, where the salt-and-pepper noise makes it difficult to identify and map different vegetation types accurately²¹. Therefore, it is important to be aware of this issue and take steps to minimize its effects in remote sensing studies. One solution could be the utilization of machine

learning algorithms, which have enabled the automatic classification of vast amounts of data with high accuracy, thereby facilitating the extraction of valuable information from remote sensing data²². The algorithms can learn from a vast amount of training data and identify patterns and relationships that are not easily discernible with traditional classification methods. This capability makes it possible to extract valuable information from UAV data, which can be used to monitor and manage mangrove forests more effectively.

Numerous ecological studies have used UAVs to analyze mangrove forests during the last decade²³. However, the outcomes of these studies have shown varying results, which largely depend on the species of mangroves being analyzed, geographical location, and the UAV platform used. For example, the initial studies analyzed multispectral²⁴ and visible²⁵ indices, leaf area index²⁶, and LiDAR²⁷. More recently, UAV data were used to quantify aboveground carbon stocks²⁸ and mangrove biomass²⁹, detect flooded areas³⁰, and classify mangrove forests at the species level³¹.

This research aimed to classify mangrove forest canopy using a series of images from a UAV and machine learning algorithms. It is expected that the seasonal canopy pattern may differ depending on the physiognomic conditions of the mangroves and the time of year when the UAV sensor collects the data. Therefore, the accuracy of species-level classifications using machine learning algorithms in mangrove forests is expected to vary over time, probably due to changes in environmental conditions, such as rainfall patterns.

Materials and Methods

Study area

The study was conducted in the Urias coastal lagoon in Mazatlán, Mexico (Fig. 1). This coastal lagoon supports four mangrove species, namely black mangrove (*Avicennia germinans*), white mangrove (*Laguncularia racemosa*), red mangrove (*Rhizophora mangle*), and buttonwood (*Conocarpus erectus*)³². Various factors influence the distribution of these mangroves in the Urias system, but salinity and hydroperiod are considered fundamental³³. For instance, the mangroves can be divided into three zones concerning the mean sea level: *Rhizophora mangle* is usually found at the lowest levels between -15.8 cm and 55.2 cm, *Laguncularia racemosa* is between 55.2 cm and 60 cm, and *Avicennia germinans* is located in the highest part between 60.7 cm and 68.2 cm³⁴.

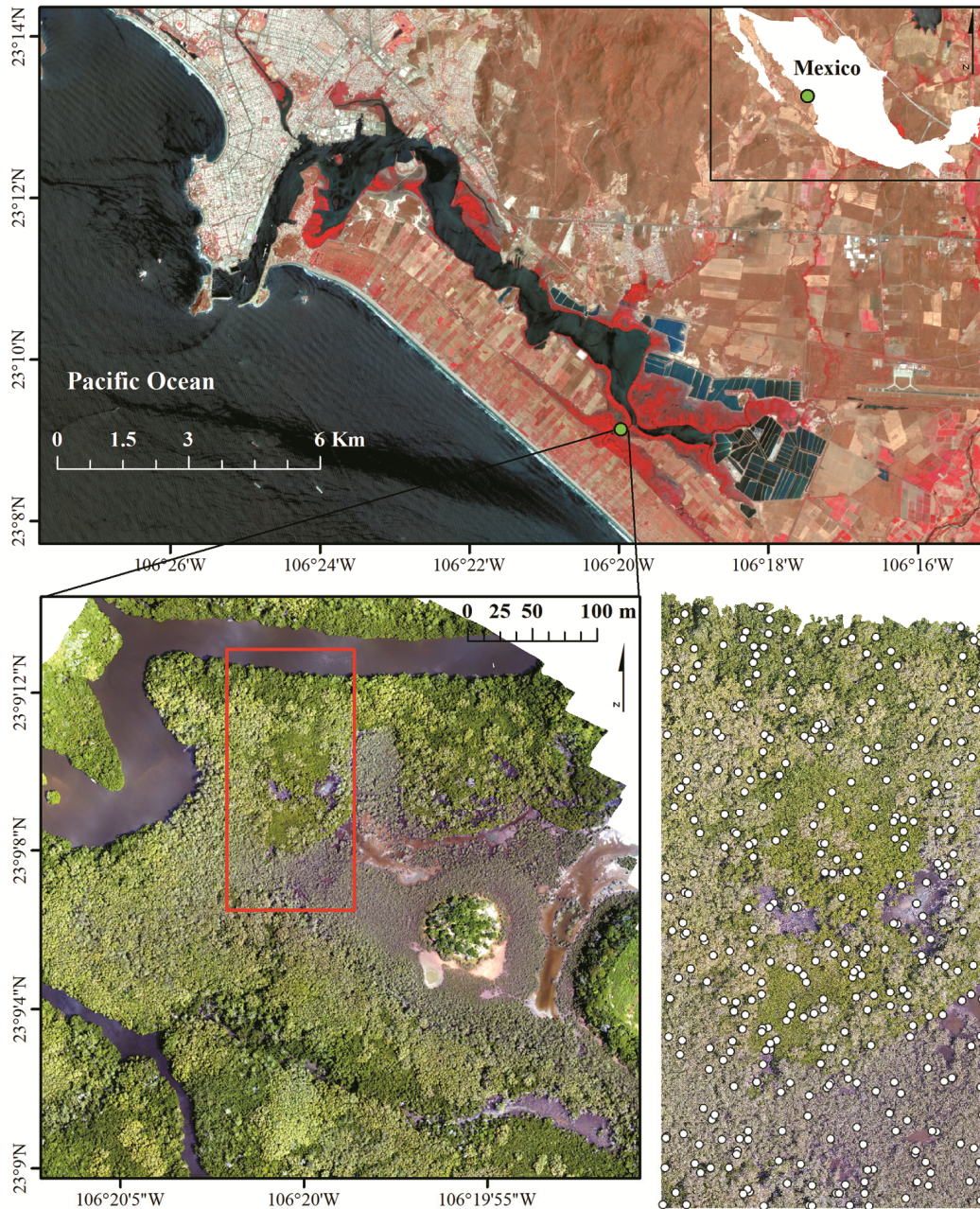


Fig. 1 — Urias coastal lagoon southeast of the Mazatlan harbour, Pacific coast of Mexico. The upper figure corresponds to a false-colour composite PlanetScope image (near-infrared, red, green) dated 25 April 2023. The lower left figure indicates the location of the UAV flights (red rectangle), and the lower right figure is the location of the 360 ground control points within the red rectangle

UAV data collection and analysis

The platform used to capture the images was a portable DJI Phantom-3 Professional with its embedded RGB camera. Flights were scheduled monthly for a year, starting in September 2018. The flight plan was programmed in an area of two hectares using the software Map Pilot installed on an iOS tablet, which automatically captures images at a height of 120 m using a longitudinal and lateral image

overlap of 70 %^(ref. 15). The images are calibrated using black and white targets in the takeoff zone. To generate the orthomosaic, traditional steps are followed in Agisoft Metashape software. These steps include image alignment, dense cloud generation, and geometric correction —using ten ground control points deployed on the field and creating and exporting the digital surface model and the orthomosaic¹⁶.

In this study, four classes were selected for classifications, including the three previously described mangrove species and an additional class called saltpan, which has no vegetation. To assess the distinctiveness of the thematic classes, a comparative analysis of the frequency histograms for each band was carried out using three regions of interest for each class. Additionally, the original RGB images were tested for improvement according to a band normalization based on the equation suggested by Zhang³⁵:

$$R_n = R/(R+G+B) \quad \dots (1)$$

$$G_n = G/(R+G+B) \quad \dots (2)$$

$$B_n = B/(R+G+B) \quad \dots (3)$$

Where, R , G , and B correspond to the original red, green, and blue channels, respectively. R_n , G_n , and B_n indicated the new normalized bands.

Machine learning algorithms

Due to the expected ultra-high spatial resolution of the orthomosaics (5.6 cm/pixel), the images were pre-analyzed with an 11×11 Lee Sigma speckle filter on SNAP to diminish the salt-and-pepper effect¹⁸. The Lee Sigma filter was used for its simplicity and effectiveness in noise reduction compared with other stationary multiplicative speckle model filters such as Lee, Kuan, and Frost³⁶. From this pre-analysis, three machine learning algorithms were applied. In essence, machine learning uses a data set of several samples of the same characteristics or attributes to predict the unknown characteristics or attributes of the data.

The Support Vector Machine (SVM) algorithm is a supervised learning method that can be used for classification, regression, and outlier detection. SVM works by finding the hyperplane that maximizes the margin between the different classes in the feature space. This hyperplane is then used to classify new data points based on their position relative to the hyperplane. SVM is particularly useful in remote sensing because it can handle high-dimensional data with a relatively small sample size³⁷. It is also robust to noise and outliers, common in remote sensing data. Additionally, SVM can take advantage of non-linear relationships between the input variables by using kernel functions to transform the input space into a higher-dimensional space where a linear hyperplane can be found.

The Artificial Neural Network (ANN) algorithm is based on the structure and function of biological neurons and synapses in the human brain, and they

are capable of learning patterns and relationships in complex data sets. ANNs can process a large amount of data and extract relevant features, which makes them suitable for handling multidimensional remote sensing data³⁸. The basic structure of an ANN consists of an input layer, one or more hidden layers, and an output layer. Each layer contains a set of neurons, and the connections between neurons are weighted to reflect the strength of the relationship between them. During the training phase, the weights are adjusted based on the error between the predicted and actual outputs. This process is repeated until the error is minimized and the network can accurately predict the output for new input data.

The Random Forest (RF) algorithm is a popular machine-learning method in remote sensing applications. It is a type of ensemble learning algorithm that combines multiple decision trees to improve the accuracy of predictions³⁹. The algorithm works by randomly selecting subsets of the training data and building decision trees based on these subsets. Each decision tree is trained on a different subset of data, which helps to reduce overfitting and increase the ability to generate the model. The final prediction is made by combining the predictions of all the individual trees in the forest¹⁹.

To evaluate the accuracy of a classification method, a confusion matrix was utilized to derive the overall accuracy and kappa statistics for each classification and season, with 90 random sampling points per class. The accuracies achieved are then compared to each other to determine the significance of the classifications using an analysis of variance (ANOVA) at a 95 % confidence level.

Results

Only eight monthly flights could be performed because the flight scheduled for January 2019 was impossible due to a cold front. Furthermore, the flights programmed for March through June 2019 were cancelled due to a security issue (Fig. 2). The horizontal Root Mean Square Error (RMSE) of the eight orthomosaics varied between 0.56 and 1.09 m. Despite having eight complete cloud-free orthomosaics, only three were used in the contrasting seasons. This decision is based on a recent phenological study of the mangrove forest in the same area using multispectral time series⁴⁰. Based on this work, the month of December 2018 was selected for the Winter Season (WS), the month of July 2019 for the Dry Season (DS), and the month of September 2019 for the Rainy Season (RS).

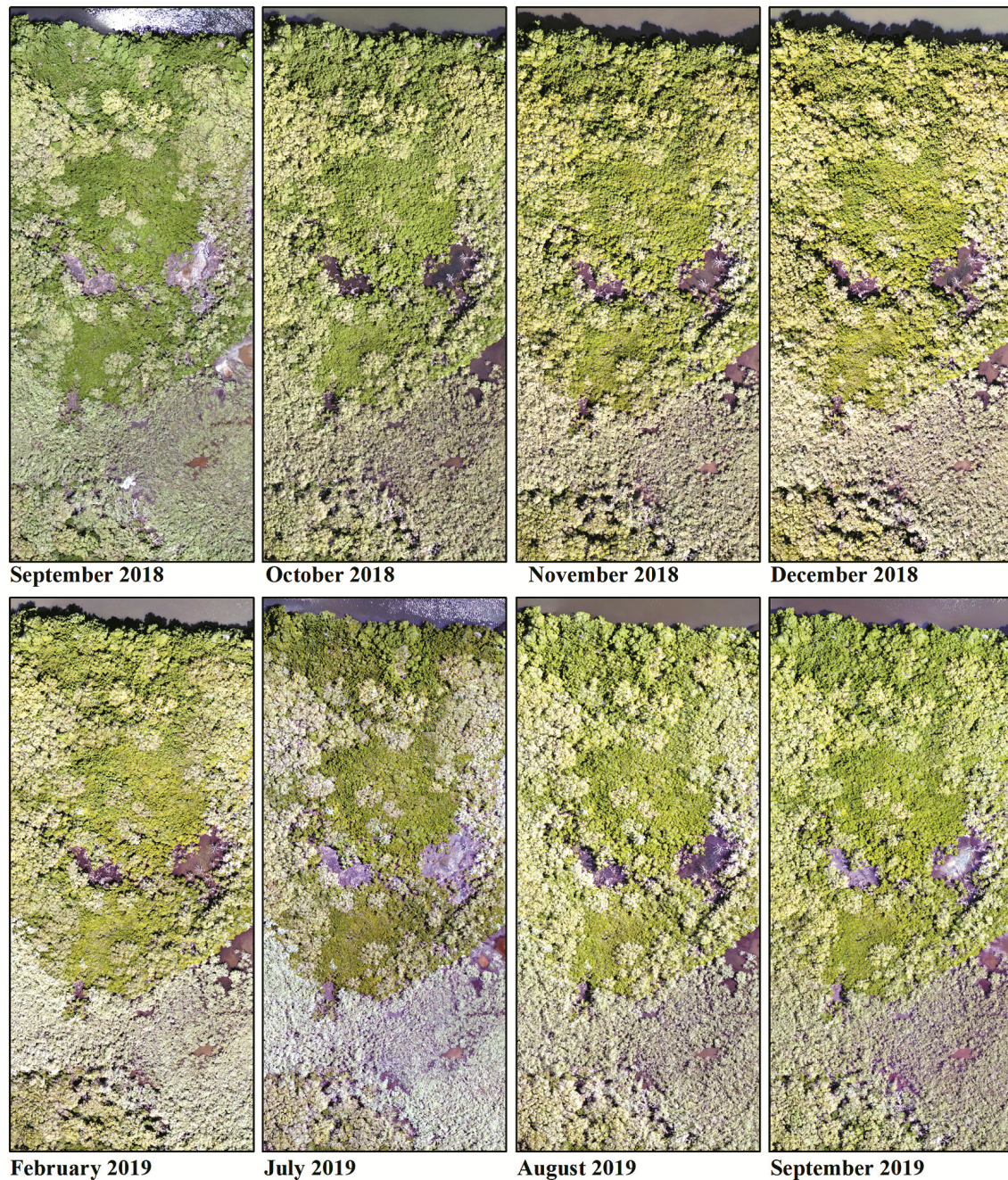


Fig. 2 — Orthomosaics derived from the UAV flights

Based on the normalized RGB data, the SVM outperformed the RF and NN in terms of overall accuracy during the data analysis phase. Specifically, the SVM algorithm achieved an accuracy of 85 % for DS, 61 % for WS, and 57 % for RS, while the RF algorithm achieved accuracies of 80 % for DS, 77 % for RS, and 63 % for WS. The NN algorithm, on the other hand, recorded accuracies of 71 % for DS, 65 % for RS, and 57 % for WS.

In a certain area within the 2-ha study site, where only *Rhizophora mangle* and saltpan classes are present (Fig. 3), the three machine learning algorithms added a new class — *Laguncularia racemosa* during the rainy season. During the dry season, RS was the only algorithm that included *Laguncularia racemosa*, while in the winter season, both RS and ANN misidentified *Rhizophora mangle* as *Laguncularia racemosa*. Finally, the SVM algorithm did not

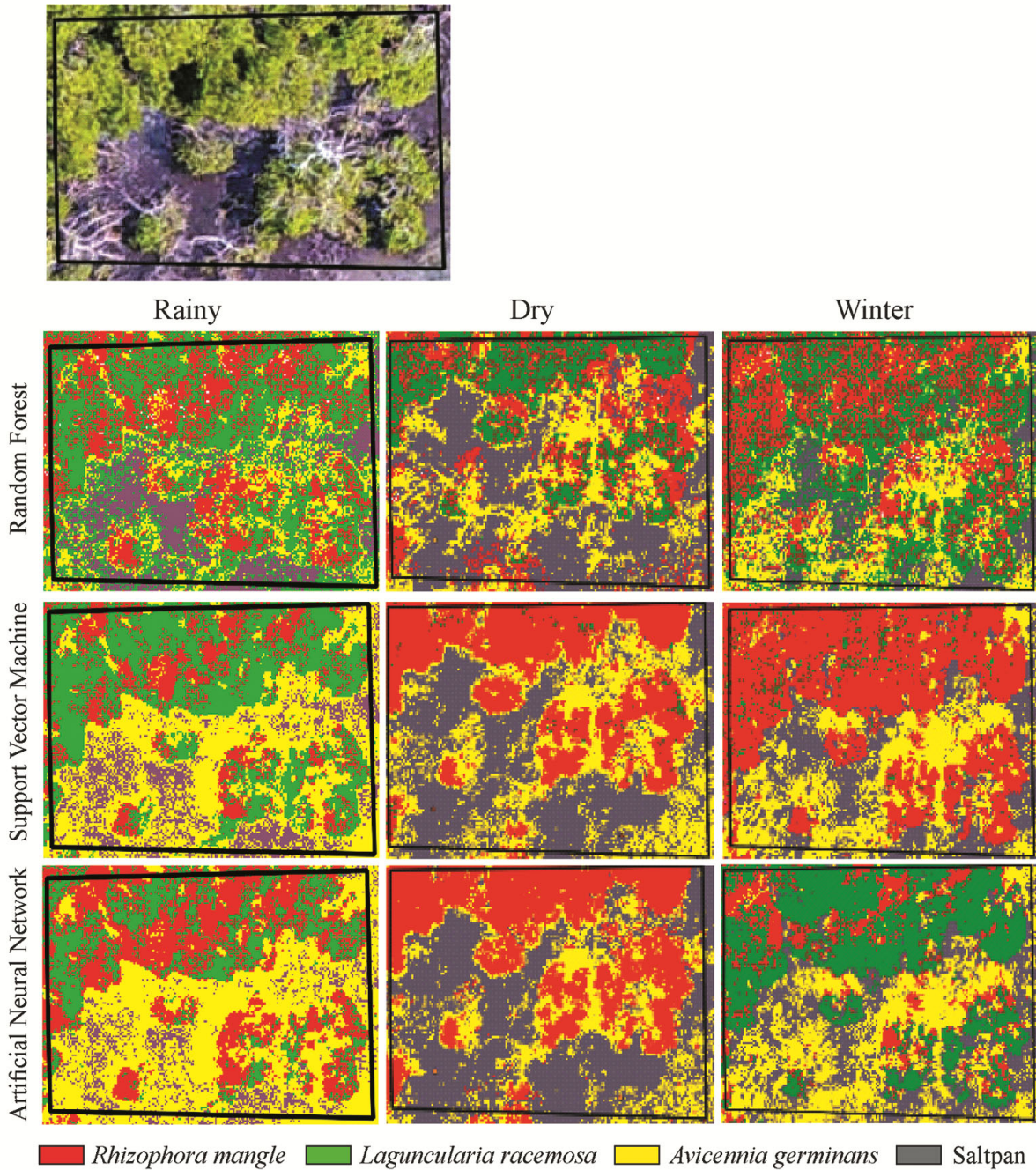


Fig. 3 — Classification outcomes of three machine-learning algorithms utilized during three different seasons in a representative section of the study area. The upper subimage represents the RGB orthomosaic

identify *Laguncularia racemosa* during the winter season, but it was the most accurate in describing the distribution of *Rhizophora mangle* during the dry season. These results indicate that utilizing the SVM algorithm could potentially improve the accuracy and efficiency of mapping the distribution of various mangrove species in the surrounding area.

When considering only the DS (Fig. 4), it has been observed that normalizing the RGB data can enhance class separation in the red and green channels. However, normalization may reduce separation in the blue channel. This decline is particularly noticeable with the two mangrove species, *Rhizophora mangle* and *Laguncularia racemosa*, which show the least

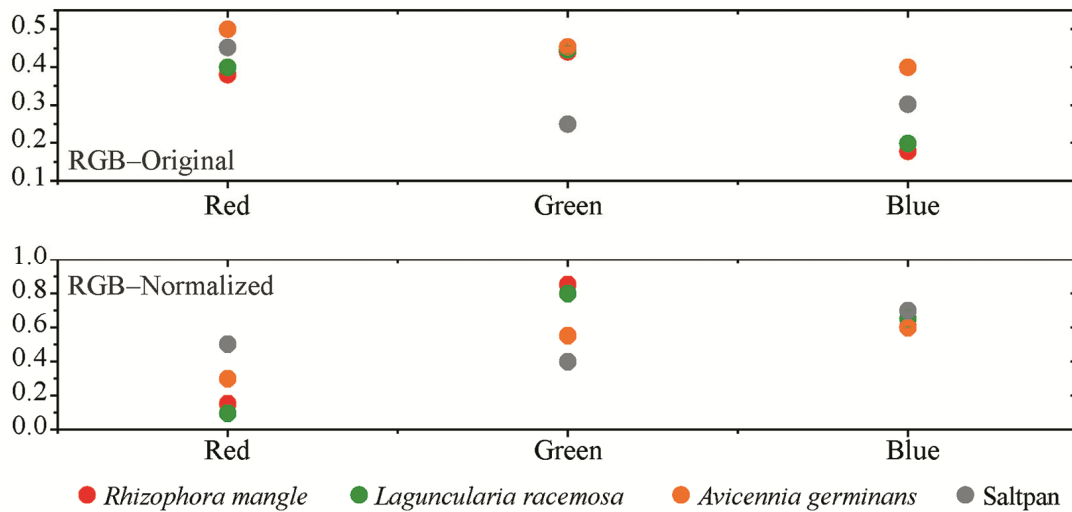


Fig. 4 — The reflectance of the original and normalized RGB orthomosaic channels for each analyzed class during the dry season

differentiation compared to other classes, regardless of the input data.

Discussion

Multispectral cameras have become increasingly popular in UAV studies as they capture detailed images of various wavelengths. However, one major issue that UAV operators are currently facing is the high cost of these cameras³². This cost can be prohibitive for many operators, particularly those with smaller budgets. One possible solution to this problem is to use lower-cost visible RGB cameras designed specifically for UAVs. These cameras may have fewer sensors or lower resolution, but they can still provide valuable data for many applications in the field of forestry¹⁵.

Due to the spectral limitations of RGB sensors, the use of learning algorithms has helped to improve classifications compared to traditional algorithms by extracting useful information from large volumes of UAV imagery³³. However, one of the major challenges faced by these algorithms is the accurate identification and classification of shadows present in the images³⁴. This situation was found in the orthomosaics of the mangrove forest in all seasons, mainly between the saltpan and *Avicennia germinans* interface. Shadows can vary in size, shape, and intensity depending on the time of day, season, and terrain, making their detection and classification difficult. One solution could be to fly when the zenith of the Sun is at its maximum and avoid shadows; however, at latitude of 23 degrees north, shadows were still present even at that time.

Colour is critical in orthomosaic classification as it works with visible images. For example, in the orthomosaics of the mangrove forest, the colour green was the dominant colour, and the algorithm used this information to identify some mangrove species and distinguish them from other landscapes, such as saltpan. *Avicennia germinans* had the least intense green colouration, making distinguishing from other mangrove species easier. However, the discrimination between *Rhizophora mangle* and *Laguncularia racemosa* proved to be more challenging. These difficulties have been previously described with the same species using spectroscopy data⁴¹. While colour is an essential component of RGB image classification, it is suggested to use this data in combination with other features, such as texture elements, to classify visible UAV data accurately.

During the transition between the end of the dry season and the beginning of the tropical storms and hurricanes, substantial discrimination was observed among mangrove classes, with the highest discrimination recorded in July for all three algorithms. A possible explanation could be that this season is characterized by strong canopy differences due to high litterfall rates in semiarid *Rhizophora mangle*⁴², *Avicennia germinans*⁴³, and *Laguncularia racemosa*⁴⁴. Moreover, the hyperspectral separation of semiarid mangroves at the leaf level is also ideal during this period³⁵. Furthermore, Asbridge *et al.*⁴⁵ found that a decrease in reflectance during the dry season can be directly linked to canopy stress and the start of senescence, pointing to mangrove physiological stress for some genera such as

Avicennia and thus achieving accurate classification results.

The identification of the saltpan class, characterized by the unique colouration that distinguishes it from the canopies of the three main mangrove species, namely *Rhizophora mangle*, *Avicennia germinans*, and *Laguncularia racemosa*, was a relatively straightforward task. Specifically, separating the red and green channels in the RGB histograms further facilitated this process. However, identifying *Avicennia germinans* presented a considerable challenge due to the faint colouration of its leaves⁴⁶, making it difficult to differentiate from the surrounding saltpan areas. Similarly, there have been reports that the saltpan and water classes can be easily identified in ALOS PALSAR¹⁸ and ALOS-2⁴⁷ radar images due to the marked difference in the backscatter of the signal between the saltpan and the mangrove canopy.

There are also some challenges associated with the use of visible UAV data with machine learning algorithms. One of the main issues is the sheer volume of data that needs to be processed²². Ultra-high-spatial resolution images can take up a lot of storage space and require substantial processing power to analyze. Additionally, the accuracy of machine learning algorithms can be affected by factors such as lighting conditions, weather, and the angle of the UAV, as seen in the different ortho images used during the year.

A key goal in using machine learning algorithms for mangrove species classification is to ensure that the algorithms are accurate and reliable³⁷. This requires careful training and validation data selection and accurate algorithm parameters selection to ensure that it does not over-fit the data or makes incorrect classifications⁴⁸. Despite these challenges, machine learning algorithms offer a powerful tool for mangrove species classification. They are expected to become increasingly important as more data is available and algorithms become more sophisticated. With the help of these algorithms, researchers can gain a deeper understanding of mangrove ecosystems and the species that inhabit them, which can be critical for conservation efforts and for understanding the impacts of climate change on these important ecosystems.

Conclusion

Based on the results, the SVM algorithm achieved an accuracy of 85 % for DS, 61 % for WS, and 57 % for RS. In comparison, the RF algorithm achieved accuracies of 80 % for DS, 77 % for RS, and 63 % for

WS, and the ANN algorithm recorded accuracies of 71 % for DS, 65 % for RS, and 57 % for WS. The findings of this study indicate that the SVM algorithm proves to be a more appropriate and effective approach for classifying UAV-based mangrove data at the pixel level, particularly during the dry season. The efficiency of the SVM in handling complex visible UAV datasets enables accurate identification and differentiation of the three mangrove species, showcasing its potential as a feasible tool in ecological monitoring. It is important to note that, despite normalizing the RGB channels and applying the speckle filter, the visible data showed minimal differentiation between the *Rhizophora mangle* and *Laguncularia racemosa* species. Thus, it is recommended to use multispectral data, particularly from the near-infrared channels. The findings provide valuable insights into the capabilities and limitations of the machine learning algorithms in the context of mangrove analysis.

Acknowledgements

PAPIIT (Mexico) provided funding for this investigation under grant No. IA100218 and IN226724 awarded to FFdS. Torres-Aguirre acknowledges grant No. 1039859 provided by CONACYT (Mexico). R Rodríguez-Sobreyra helped during the initial stage of the investigation.

Conflict of Interest

No potential conflict of interest was reported by the authors.

Data Availability

The data supporting this study's findings are available from the corresponding author [FFdS], upon reasonable request.

Authors Contributions

ETA: Conceptualization, data curation, methodology, visualization, and writing—original draft preparation; FFdS: Formal analysis, writing—review & editing, and funding acquisition; LVL: Conceptualization, data curation, software, and validation; FA: Investigation, and supervision; and FFV: Investigation, supervision, and validation.

References

- 1 Aji M A P, Kamal M & Farda N M, Mangrove species mapping through phenological analysis using random forest algorithm on Google Earth Engine, *Remote Sens Appl: Soc Environ*, 30 (2023) p. 100978. <https://doi.org/10.1016/j.rsase.2023.100978>

- 2 Beselley S M, Grueters U, Wegen M V D, Reynolds J, Dijkstra J, *et al.*, Modelling mangrove-mudflat dynamics with a coupled individual-based-hydro-morphodynamic model, *Environ Model Softw*, 169 (2023) p. 105814. <https://doi.org/10.1016/j.envsoft.2023.105814>
- 3 Serrano D, Flores-Verdugo F, Ramírez-Félix E, Kovacs J M & Flores-de-Santiago F, Modeling tidal hydrodynamic changes induced by the opening of an artificial inlet within a subtropical mangrove dominated estuary, *Wetl Ecol Manag*, 28 (2020) 103–118. <https://doi.org/10.1007/s11273-019-09697-w>
- 4 Muro-Torres V, Amezcua F, Ramírez-Ortiz G, Flores-de-Santiago F, Amezcua-Linares F, *et al.*, Assessing the spatiotemporal relationship between coastal habitats and fish assemblages at two neotropical estuaries of the Mexican Pacific, *Diversity*, 14 (8) (2022) p. 619. <https://doi.org/10.3390/d14080619>
- 5 Chowdhury P, Lakku N K G, Lincoln S, Seelam J K & Behera M R, Climate change and coastal morphodynamics: Interactions on regional scales, *Sci Total Environ*, 899 (2023) p. 166432. <https://doi.org/10.1016/j.scitotenv.2023.166432>
- 6 Radabaugh K R, Moyer R P, Chappel A R, Breithaupt J L, Lagomasino D, *et al.*, A spatial model comparing above- and belowground blue carbon stocks in Southwest Florida mangroves and salt marshes, *Estuar Coast*, 46 (2023) 1536–1556. <https://doi.org/10.1007/s12237-023-01217-7>
- 7 Rogers K, Adams J, Cormier N, Kelleway J & Saintilan N, Climate change effects on intertidal and subtidal environments: Impacts, projections, and management, In: *Climate Change and Estuaries*, edited by Kennish M J, Paerl H W & Crosswell J R, (CRC Press, USA), 2023, pp. 249–274. <http://dx.doi.org/10.1201/9781003126096-15>
- 8 Apostolopoulos D & Nikolakopoulos K, A review and meta-analysis of remote sensing data, GIS methods, materials and indices used for monitoring the coastline evolution over the last twenty years, *Eu J Remote Sens*, 54 (1) (2021) 240–265. <https://doi.org/10.1080/22797254.2021.1904293>
- 9 Sun W, Chen C, Liu W, Yang G, Meng X, *et al.*, Coastline extraction using remote sensing: a review, *GISci Remote Sens*, 60 (1) (2023) p. 2243671. <https://doi.org/10.1080/15481603.2023.2243671>
- 10 Vizcaya-Martínez D A, Flores-de-Santiago F, Valderrama-Landeros L, Serrano D, Rodríguez-Sobreyra R, *et al.*, Monitoring detailed mangrove hurricane damage and early recovery using multisource remote sensing data, *J Environ Manag*, 320 (2022) p. 115830. <https://doi.org/10.1016/j.jenvman.2022.115830>
- 11 Dronova I, Kislik C, Dinh Z & Kelly M, A review of unoccupied aerial vehicle use in wetland applications: emerging opportunities in approach, technology, and data, *Drones*, 5 (2021) p. 45. <https://doi.org/10.3390/drones5020045>
- 12 Minervino Amodio A, Di Paola G & Roskopf C M, Monitoring coastal vulnerability by using DEMs based on UAV spatial data, *ISPRS Int J Geo-Inf*, 11 (2022) p. 155. <https://doi.org/10.3390/ijgi11030155>
- 13 Novais J, Vieira A, Bento-Gonçalves A, Silva S, Folharini S, *et al.*, The use of UAVs for morphological coastal change monitoring—A bibliometric analysis, *Drones*, 7 (2023) p. 629. <https://doi.org/10.3390/drones7100629>
- 14 Li Q, Wong F K K, Fung T, Brown L A & Dash J, Assessment of active LiDAR data and passive optical imagery for double-layered mangrove leaf area index estimation: A case study in Mai Po, Hong Kong, *Remote Sens*, 15 (2023) p. 2551. <https://doi.org/10.3390/rs15102551>
- 15 Flores-de-Santiago F, Valderrama-Landeros L, Rodríguez-Sobreyra R & Flores-Verdugo F, Assessing the effect of flight altitude and overlap on orthoimage generation for UAV estimates of coastal wetlands, *J Coast Conserv*, 24 (2020) p. 35. <https://doi.org/10.1007/s11852-020-00753-9>
- 16 Flores-de-Santiago F, Valderrama-Landeros L, Villaseñor-Aguirre J, Álvarez-Sánchez L F, Rodríguez-Sobreyra R, *et al.*, Detection of beach-dune geomorphic changes by means of satellite and UAV data: The case of Altamura Island in the Gulf of California, *Coasts*, 3 (4) (2023) 383–400. <https://doi.org/10.3390/coasts3040023>
- 17 Nikolakopoulos K, Kyriou A, Koukouvelas I, Zygouri V & Apostolopoulos D, Combination of aerial, satellite, and UAV photogrammetry for mapping the diachronic coastline evolution: The case of Lefkada Island, *ISPRS Int J Geo-Inf*, 8 (2019) p. 489. <http://dx.doi.org/10.3390/ijgi8110489>
- 18 Flores-de-Santiago F, Kovacs J M & Lafrance P, An object-oriented classification method for mapping mangroves in Guinea, West Africa, using multipolarized ALOS PALSAR L-band data, *Int J Remote Sens*, 34 (2) (2013) 563–586. <http://dx.doi.org/10.1080/01431161.2012.715773>
- 19 Tsiakos C A D & Chalkias C, Use of machine learning and remote sensing techniques for shoreline monitoring: A review of recent literature, *Appl Sci*, 13 (2023) p. 3268. <https://doi.org/10.3390/app13053268>
- 20 Kim H, Yu J, Wang L, Park C, Han H S, *et al.*, Analysis on effective UAS survey conditions for classification of coastal sediments, *IEEE J Sel Top Appl Earth Obs Remote Sens*, 15 (2022) 1163–1173. <http://dx.doi.org/10.1109/JSTARS.2021.3136228>
- 21 Lausch A, Schaepman M E, Skidmore A K, Truckenbrodt S C, Hacker J M, *et al.*, Linking the remote sensing of geodiversity and traits relevant to biodiversity—Part II: Geomorphology, terrain and surfaces, *Remote Sens*, 12 (2020) p. 3690. <http://dx.doi.org/10.3390/rs12223690>
- 22 Boussetta A, Niculescu S, Bengoufa S & Zagrarni M F, Deep and machine learning methods for the (semi-)automatic extraction of sandy shoreline and erosion risk assessment based on remote sensing data (case of Jerba island -Tunisia), *Remote Sens Appl: Soc Environ*, 32 (2023) p. 101084. <https://doi.org/10.1016/j.rsase.2023.101084>
- 23 Zimudzi E, Sanders I, Rollings N & Omlin C W, Remote sensing of mangroves using unmanned aerial vehicles: current state and future directions, *J Spatial Sci*, 66 (2) (2021) 195–212. <https://doi.org/10.1080/14498596.2019.1627252>
- 24 Yu X, Liu Q, Liu X, Liu X & Wang Y, A physical-based atmospheric correction algorithm of unmanned aerial vehicles images and its utility analysis, *Int J Remote Sens*, 38 (8–10) (2017) 3101–3112. <http://dx.doi.org/10.1080/01431161.2016.1230291>
- 25 Liu X & Wang L, Feasibility of using consumer-grade unmanned aerial vehicles to estimate leaf area index in mangrove forest, *Remote Sens Lett*, 9 (11) (2018) 1040–1049. <https://doi.org/10.1080/2150704X.2018.1504339>

- 26 Tian J, Wang L, Li X, Gong H, Shi H, *et al.*, Comparison of UAV and WorldView-2 imagery for mapping leaf area index of mangrove forest, *Int J Appl Earth Obs Geoinformation*, 61 (2017) 22–31. <http://dx.doi.org/10.1016/j.jag.2017.05.002>
- 27 Guo Q, Su Y, Hu T, Zhao X, Wu F, *et al.*, An integrated UAV-borne lidar system for 3D habitat mapping in three forest ecosystems across China, *Int J Remote Sens*, 38 (8–10) (2017) 2954–2972. <http://dx.doi.org/10.1080/01431161.2017.1285083>
- 28 Li Z, Zan Q, Yang Q, Zhu D, Chen Y, *et al.*, Remote estimation of mangrove aboveground carbon stock at the species level using a low-cost unmanned aerial vehicle system, *Remote Sens*, 11 (2019) p. 1018. <http://dx.doi.org/10.3390/rs11091018>
- 29 Wang D, Wan B, Liu J, Su Y, Guo Q, *et al.*, Estimating aboveground biomass of the mangrove forests on northeast Hainan Island in China using upscaling method from field plots, UAV-LiDAR data and Sentinel-2 imagery, *Int J Appl Earth Obs Geoinformation*, 85 (2020) p. 101986. <https://doi.org/10.1016/j.jag.2019.101986>
- 30 Zhu X, Hou Y, Weng Q & Chen L, Integrating UAV optical imagery and LiDAR data for assessing the spatial relationship between mangrove and inundation across a subtropical estuarine wetland, *ISPRS J Photogram Remote Sens*, 149 (2019) 146–156. <https://doi.org/10.1016/j.isprsjprs.2019.01.021>
- 31 Wang D, Wan B, Qiu P, Tan X & Zhang Q, Mapping mangrove species using combined UAV-LiDAR and Sentinel-2 data: Feature selection and point density effects, *Adv Space Res*, 69 (2022) 1494–1512. <https://doi.org/10.1016/j.asr.2021.11.020>
- 32 Flores-de-Santiago F, Kovacs J M & Flores-Verdugo F, Seasonal changes in leaf chlorophyll a content and morphology in a sub-tropical mangrove forest of the Mexican Pacific, *Mar Ecol Prog Series*, 444 (2012) 57–68. <http://dx.doi.org/10.3354/meps09474>
- 33 Flores-de-Santiago F, Serrano D, Flores-Verdugo F & Monroy-Torres M, Application of a simple and effective method for mangrove afforestation in semiarid regions combining nonlinear models and constructed platforms, *Ecol Eng*, 103 (2017) 244–255. <http://dx.doi.org/10.1016/j.ecoleng.2017.04.008>
- 34 Flores-Verdugo F, Ramírez-Barrón E & Flores-de-Santiago F, Hydroperiod enhancement using underground pipes for the efficient removal of hypersaline conditions in a semiarid coastal lagoon, *Cont Shelf Res*, 162 (2018) 39–47. <http://dx.doi.org/10.1016/j.csr.2018.04.008>
- 35 Zhang J, Virk S, Porter W, Kenworthy K, Sullivan D, *et al.*, Applications of unmanned aerial vehicle based imagery in turfgrass field trials, *Front Plant Sci*, 10 (2019) p. 279. <http://dx.doi.org/10.3389/fpls.2019.00279>
- 36 Lee J S, Wen J H, Ainsworth T L, Chen K S & Chen A J, Improved Sigma filter for speckle filtering of SAR imagery, *IEE Trans Geosci Remote Sens*, 47 (1) (2009) 202–213. <http://dx.doi.org/10.1109/TGRS.2008.2002881>
- 37 Bengoufa S, Niculescu S, Mihoubi M K, Belkessa R, Rami A, *et al.*, Machine learning and shoreline monitoring using optical satellite images: case study of the Mostaganem shoreline, Algeria, *J Appl Remote Sens*, 15 (2) (2021) p. 026509. <http://dx.doi.org/10.1117/1.JRS.15.026509>
- 38 Valderrama-Landeros L, Flores-Verdugo F & Flores-de-Santiago F, Assessing the coastal vulnerability by combining field surveys and the analytical potential of CoastSat in a highly impacted tourist destination, *Geographies*, 2 (2022) 642–656. <https://doi.org/10.3390/geographies2040039>
- 39 Valderrama-Landeros L, Blanco y Correa M, Flores-Verdugo F, Álvarez-Sánchez L F & Flores-de-Santiago F, Spatiotemporal shoreline dynamics of Marismas Nacionales, Pacific coast of Mexico, based on a remote sensing and GIS mapping approach, *Environ Monit Assess*, 192 (2020) p. 123. <https://doi.org/10.1007/s10661-020-8094-8>
- 40 Valderrama-Landeros L, Flores-Verdugo F, Rodríguez-Sobreyra R, Kovacs J M & Flores-de-Santiago F, Extrapolating canopy phenology information using Sentinel-2 data and the Google Earth Engine platform to identify the optimal dates for remotely sensed image acquisition of semiarid mangroves, *J Environ Manage*, 279 (2021) p. 111617. <https://doi.org/10.1016/j.jenvman.2020.111617>
- 41 Flores-de-Santiago F, Kovacs J M, Wang J, Flores-Verdugo F, Zhang C, *et al.*, Examining the influence of seasonality, condition, and species composition on mangrove leaf pigment contents and laboratory based spectroscopy data, *Remote Sens*, 8 (2016) p. 226. <http://dx.doi.org/10.3390/rs8030226>
- 42 Félix-Pico E F, Holguín-Quinones O E, Hernández-Herrera A & Flores-Verdugo F, Mangrove primary production at El conchalito estuary in La Paz Bay (Baja California Sur, Mexico), *Ciencias Marinas*, 32 (1A) (2006) 53–63. <https://doi.org/10.7773/cm.v32i1.65>
- 43 Arreola-Lizárraga J A, Flores-Verdugo F J & Ortega-Rubio A, Structure and litterfall of an arid mangrove stand on the Gulf of California, Mexico, *Aquat Bot*, 79 (2004) 137–143. <https://doi.org/10.1016/j.aquabot.2004.01.012>
- 44 Flores-Verdugo F J, Day J W & Briseno-Dueñas R, Structure, litterfall, decomposition, and detritus dynamics of mangroves in a Mexican coastal lagoon with an ephemeral inlet, *Mar Ecol Prog Ser*, 35 (1987) 83–90. <https://www.jstor.org/stable/24825012>
- 45 Asbridge E F, Bartolo R, Finlayson C M, Lucas R M, Rogers K, *et al.*, Assessing the distribution and drivers of mangrove dieback in Kakadu National Park, northern Australia, *Estuar Coast Shelf Sci*, 228 (2019) p. 106353. <https://doi.org/10.1016/j.ecss.2019.106353>
- 46 Flores-de-Santiago F, Kovacs J M & Flores-Verdugo F, Discrimination of 3 dominant mangrove species from the Pacific coast of Mexico by spectroscopy on intact leaves, *Ciencias Marinas*, 44 (3) (2018) 185–202. <http://dx.doi.org/10.7773/cm.v44i3.2806>
- 47 Karimzadeh S, Kamran K V & Mahdavi-fard M, A multisensory satellite image classification for the detection of mangrove forests in Qeshm Island (Southern Iran), *Appl Geomatics*, 15 (2023) 177–188. <https://doi.org/10.1007/s12518-022-00475-7>
- 48 Apostolopoulos D N & Nikolakopoulos K G, Assessment and quantification of the accuracy of low-and high-resolution remote sensing data for shoreline monitoring, *ISPRS Int J Geo-Inf*, 9 (2020) p. 391. <http://dx.doi.org/10.3390/ijgi9060391>